Hindawi
Mathematical Problems in Engineering
Volume 2018, Article ID 7439137, 13 pages
https://doi.org/10.1155/2018/7439137

Research Article

Analyses and Control of Chaotic Behavior in DC-DC Converters

Cheng-Biao Fu,[1] An-Hong Tian,[1] Kuo-Nan Yu,[2] Yi-Hung Lin,[2] and Her-Terng Yau[2]

[1]*College of Information Engineering, Qujing Normal University, Qujing 655011, China*
[2]*National Chin-Yi University of Technology, Taichung 41170, Taiwan*

Correspondence should be addressed to Her-Terng Yau; pan1012@ms52.hinet.net

Received 11 April 2018; Revised 26 September 2018; Accepted 21 October 2018; Published 8 November 2018

Academic Editor: Francesco Riganti-Fulginei

In this study the nonlinear behavior of a buck converter was simulated and the responses of Phases 1 and 2 and the chaotic phase were investigated using changes of input voltage. After a dynamic system model had been acquired using basic electronic circuit theory, Matlab and Pspice simulations were used to study system inductance, resistance, and capacitance. The characteristic changes of input voltage, and phase plane traces from simulation and experiments showed nonlinear behavior in Phases 1 and 2, as well as a chaotic phase. PID control and Integral Absolute Error (IAE) were used as adaption coefficients to control chaotic behavior, and particle swarm optimization (PSO) and the genetic algorithm were used to find the optimal gain parameters for the PID controller. Simulation results showed that the control of chaotic phenomena could be achieved and errors were close to zero. Fuzzy control was also used effectively to prevent chaos. The experimental results also showed nonlinear behavior from Phases 1 and 2 as well as the chaotic phase. Laboratory experiments conducted using both PID and fuzzy control echoed the simulation results. The fuzzy control results were somewhat better than those obtained with PID.

1. Introduction

DC-DC converters are very common and can be found in almost all the electronic devices in everyday use: PCs, Pads, mobile phones, TVs, and other types of equipment. The need for the delivery of finely tuned stable voltages by these devices makes it necessary for them to be of high quality. However, a review of the literature showed that abnormal or irregular behavior is often a characteristic of DC-DC converters [1] and this includes electromagnetic noise and critical operation breakdown. A previous study [2] using nonlinear dynamic theory, numerical computation, and experimental circuitry revealed the presence of nonlinear bifurcation behavior in many of these converters.

In a power conversion system, DC-DC converters are basic modules that include inductors (L), capacitors (C), switches (S), and diodes (D). Different connection arrangement gives different topological structure to achieve the various purposes of power treatment or the format of the transformation required. The DC-DC converters discussed here include buck converters, boost converters, and buck-booster converters.

Control of a DC-DC converter is achieved by a voltage or current signal. The operation of such circuits is often associated with irregular and unstable chaotic behavior similar to noise [3]. These phenomena are often ignored, but these nonlinear oscillations consume system energy and lower the efficiency of the converter.

DC-DC converters operate within a certain range of input voltage, and a phase plane diagram will show the changes that occur over the range [4–6]. This limits the conditions of use to a significant degree. To improve this situation, the converter was viewed as a controlled body and various control theories were added so that it could be used to return the system to stability when chaos arose.

Matlab and Pspice simulations of the behavior of the buck converter chosen for this study showed that the stable dynamic trace of output in the phase plane diagram against changes of input voltage later becomes chaotic.

We cut in from a control perspective. In the past, there were many commonly used control rules. Traditionally, these rules have used PID system controllers [7, 8], but recently many rules using optimization to implement automatic parameter settings have been presented. However, most

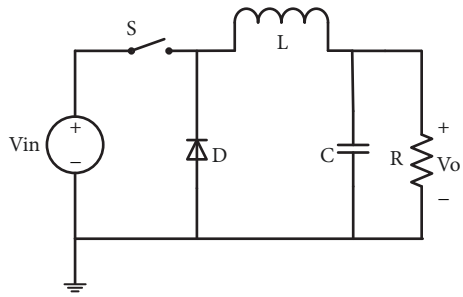

Figure 1: The basic circuit of a buck converter.

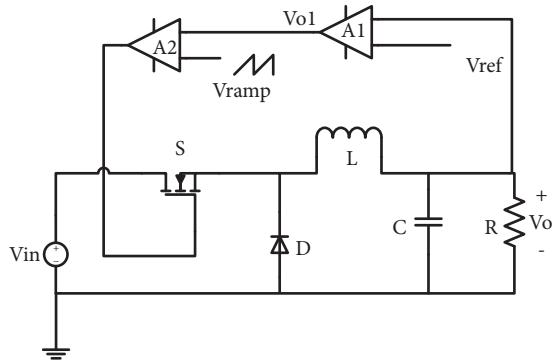

Figure 2: Buck converter feedback circuit.

optimization algorithms fall into the local optimum trap. To avoid this type of situation some investigators have used a chaos logistic map to improve optimization [9, 10].

To better understand and achieve control of this phenomenon, optimization algorithms were used: the particle swarm optimization algorithm (PSO) [11], the Genetic algorithm (GA) [12], and fuzzy control (Fuzzy control) [13]. Phase plane diagrams, power spectra, and the Lyapunov exponent were used to display the results of system status analysis.

Section 2 of this paper describes system structure and analyzes and derives system equations. In Section 3 the equations derived in Section 2 were used to construct a block diagram and conduct a Pspice simulation. Changes in input voltages are clearly reflected in changes in the phase plane diagrams. Simulation results were then examined and the power spectrum and Lyapunov exponent were introduced to demonstrate the presence of chaos in the system. After the confirmation of the existence of chaos, optimization algorithms were used to look for the best PID parameters to control the chaotic behavior. Fuzzy control was included for comparison. Section 5 is the conclusion.

2. Buck Converters

Buck converters were invented at the beginning of the 20th Century. DC-DC converters were the earliest type and the principle used can be easily understood.

The structure of a buck DC-DC converter is shown in Figure 1 and the equations can be derived as follows.

Model 1. In both ON and OFF condition, Kirchhoff's Voltage (*KVL*) and Current (*KCL*) laws can be used to derive the following equations:

$$C\frac{dV_C}{dt} = i_L - \frac{V_o}{R} \tag{1}$$

$$L\frac{di_L}{dt} = uV_{in} - V_o \tag{2}$$

$$u = \begin{cases} 0, & \text{when S off} \\ 1, & \text{when S on} \end{cases} \tag{3}$$

In this study of DC-DC converters, both simulation and laboratory experiments were done using basic buck converter specifications. A feedback system was added to the voltage output that was used to send a 0 or 1 signal via the error amplifier after amplification had been done a times. A comparison was made using A_2 and the sawtooth wave V_{ramp} to feed back to S (on/off) to drop the output voltage to a certain level. Figure 2 shows a schematic of the buck converter. To start with it is assumed that all circuit components are in an ideal state. When S is ON and D is OFF, the input voltage V_{in} flows to L and R and current passes the inductance and charges the capacitor. When S is OFF and D is ON, energy stored by the inductor and capacitor via D provides feedback and releases energy to R. The feedback, V_o connected to A_1. A_1 can be regarded as gain a. After V_o is less than V_{ref} and amplified a, (4) is valid:

$$V_{o1}(t) = a\left(V_o(t) - V_{ref}\right) \tag{4}$$

When V_{o1} connects A_2 to compare the V_{ramp}, sawtooth wave, $V_{ramp} > V_{o1}$ gives a high signal to switch M_P on; conversely, if $V_{ramp} < V_{o1}$, the output signal of the comparator is Low, M_P is switched off. This nonlinear switching can result in several different kinds of system behavior.

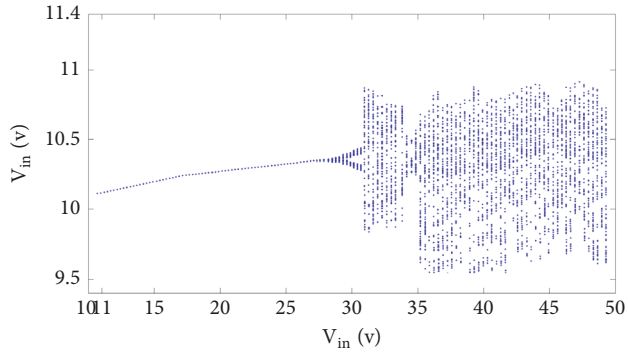

FIGURE 3: A buck converter bifurcation trace.

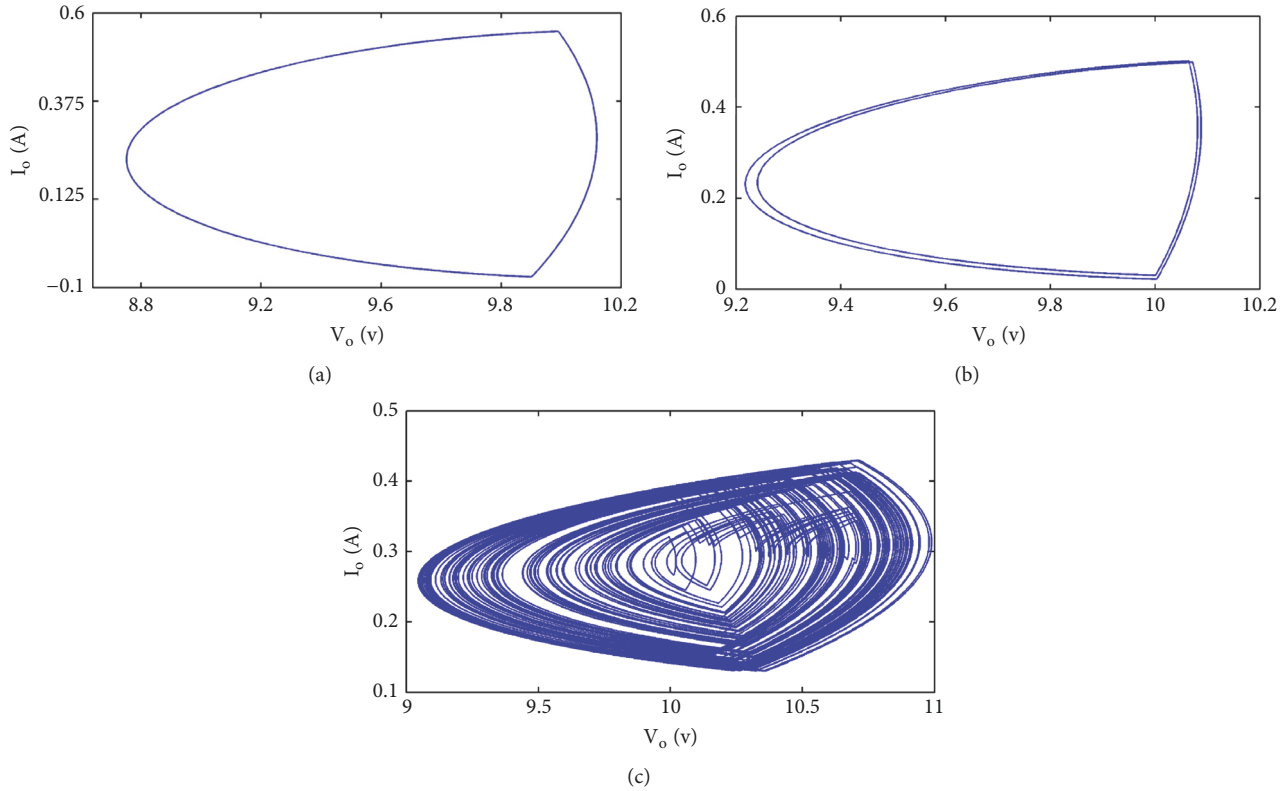

FIGURE 4: (a) $V_o - I_L$ phase plane diagram of Phase 1. (b) $V_o - I_L$ phase plane diagram of Phase 2. (c) $V_o - I_L$ phase plane diagram of the irregular phase.

3. Simulation and Analyses

3.1. Matlab Simulation. A mathematical model of a buck converter was made with Matlab/Simulink using the equations derived in Section 2, (1)-(3), and (4). The parameters used are shown in Table 1. The symbol table of this study is shown in Table 2. To start with the input voltage V_{in} was set to 11, and the buck converter behavior was stable. Figure 4(a) shows the phase plane diagram $V_o - I_o$ of Phase 1. In the next step V_{in} was gradually increased to 30, and the phase plane diagram (Phase 2) changes as shown in Figure 4(b). Finally, after the voltage was increased to 40, the converter entered an irregular phase as shown in Figure 4(c), the irregular $V_o - I_o$ phase plane diagram.

When the parameters of a nonlinear circuit are changed, an initial stable phase gradually changes and eventually become irregular. In this study the parameters selected for study and observation were those most likely to change, such as the input voltage V_{in}. All the parameters with the exception of V_{in} had a fixed value [14–16].

Figure 3 clearly shows how the system changes from Phase 1, to Phase 2, and then to irregular dynamic behavior. We used input voltages of 11, 30, and 40 for comparison.

The phase plane diagrams in Figures 4(a), 4(b), and 4(c) clearly show how the dynamic behavior of the buck converter becomes nonlinear with an increase of voltage after Phase 1.

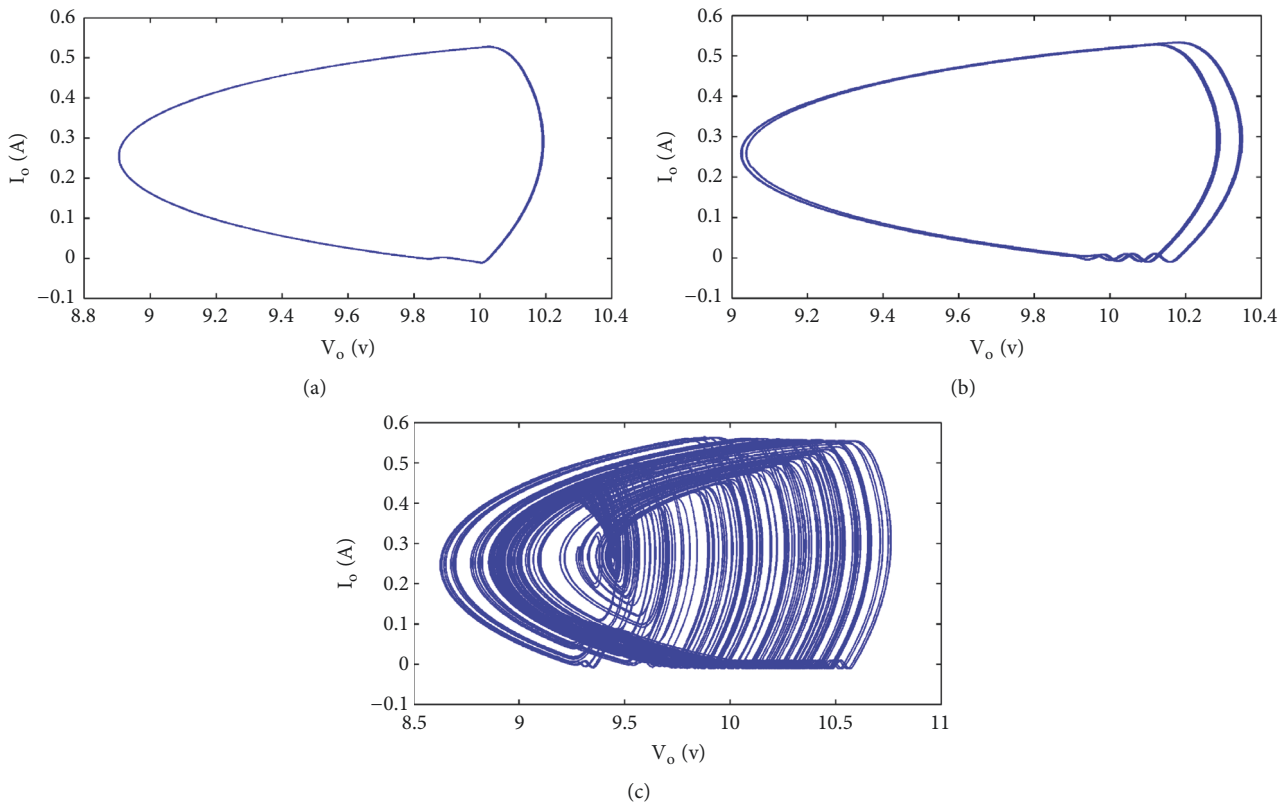

Figure 5: (a). $V_o - I_L$ phase plane diagram of Phase 1. (b). $V_o - I_L$ phase plane diagram of Phase 2. (c). $V_o - I_L$ phase plane diagram of the irregular phase.

Table 1: Parameter specification.

Parameter	Value
Vin	11~40V
L	2 m
C	47u
A1	5.6
R	35 Ω
Vref	9.4V
Vramp	4-10V
f	1 K

3.2. Pspice Simulation. A MOSFET switch at 15 V was used for the buck converter simulation using Pspice. A Zener was added at the back of A2 to increase the signal by 15 V to ensure proper operation of the switch. Figure 5(a) shows the phase 1 $V_o - I_L$ phase plane diagram with V_{in} set as 11 V in a Pspice simulation. When V_{in} was increased to 30, the $V_o - I_L$ phase plane diagram changed to Phase 2 behavior as shown in Figure 5(b). Finally, with a voltage of 40, the converter phase plane diagram displayed the irregular behavior illustrated in Figure 5(c).

Figures 5(a), 5(b), and 5(c) clearly show distinct changes from Phase 1 to Phase 2, and then to nonlinear dynamic behavior, in response to an increase of voltage.

3.3. Experimental Results. Circuit experiments are less convenient than computer simulations. For example, current cannot be directly detected. It was necessary to use a Fluke or Hall device to measure current. For resistance measurement, a high value ceramic resister was used. Figure 6 shows the buck converter circuit used in the experiments.

Figures 7(a), 7(b), and 7(c) are V0–IL plane diagrams of an oscilloscope display showing voltage as 11 V in Phase 1, 30 V in Phase 2, and 40 V in the irregular phase. The experimental setup is shown in Figure 8 and the results coincided very well with those of the simulation.

3.4. Chaos Analyses. While the phase plane diagrams clearly showed whether the behavior of the buck converter was regular or not, they did not provide information about chaos. Therefore, power spectra and the Lyapunov exponent were used in addition to phase plane diagrams to investigate chaotic behavior.

Figure 9 shows the power spectra of the converter in Phase 1, 11 V (see Figure 9(a)), Phase 2, 30 V (see Figure 9(b)), and irregular phase, 40 V (see Figure 9(c)).

Figure 10(a) shows the power spectrum diagram of Phase 1 with an input voltage of 11V. In Figure 10(b) the input voltage was 40 V and circuit behavior was nonlinear.

The Lyapunov exponent diagrams in Figures 11 and 12 show the state of the converter in Phase 1 (11V) and in a

Table 2: Symbol table.

Name	Symbol	Name	Symbol	Name	Symbol
S	Switch	R	Resistance	V_O	Output voltage
D	Diode	I_L	Inductance current	V_L	Inductance voltage
L	Inductance	I_C	Capacitance current	V_C	Capacitance voltage
C	Capacitance	V_S	Input voltage		

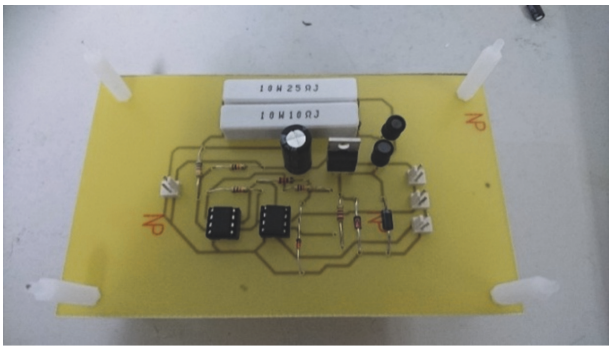

Figure 6: Physical buck converter circuit board.

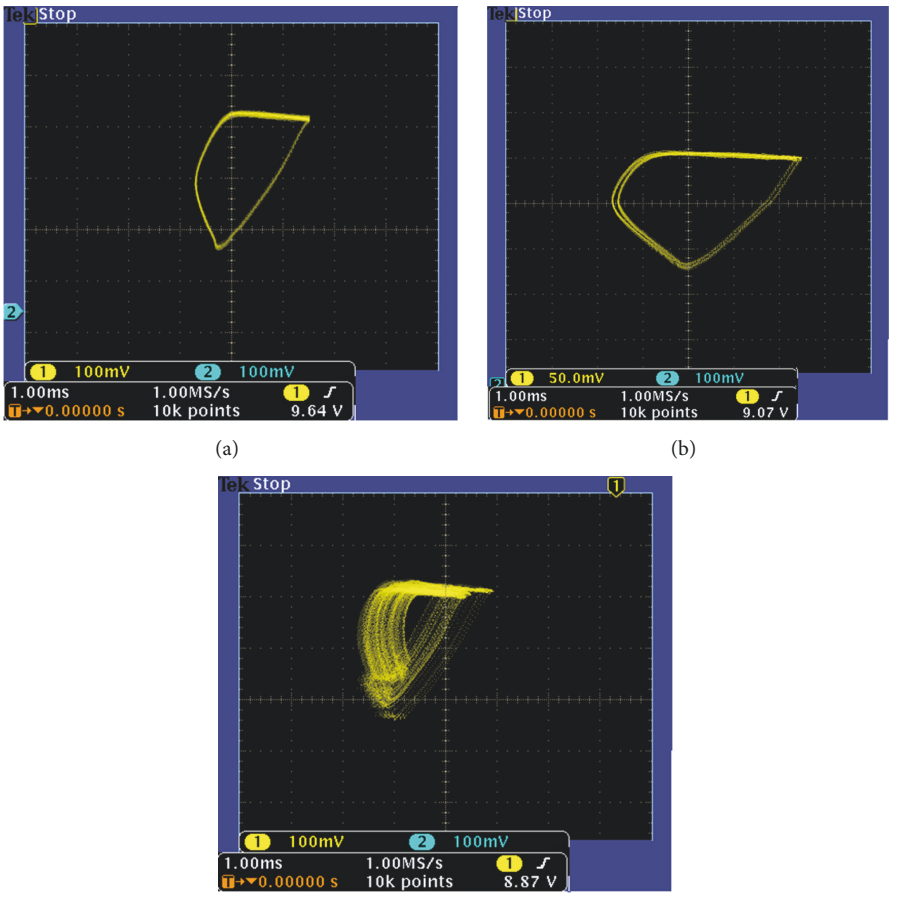

(a) (b)

(c)

Figure 7: (a) $V_o - I_L$ phase plane diagram on oscilloscope display in Phase 1. (b) $V_o - I_L$ phase plane diagram on oscilloscope display in Phase 2. (c) $V_o - I_L$ phase plane diagram on oscilloscope display in the chaotic phase.

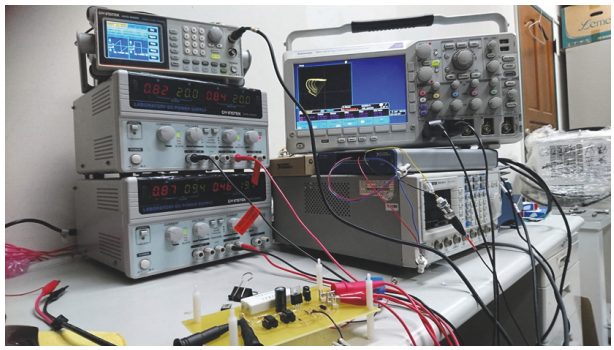

Figure 8: Laboratory experimental setup.

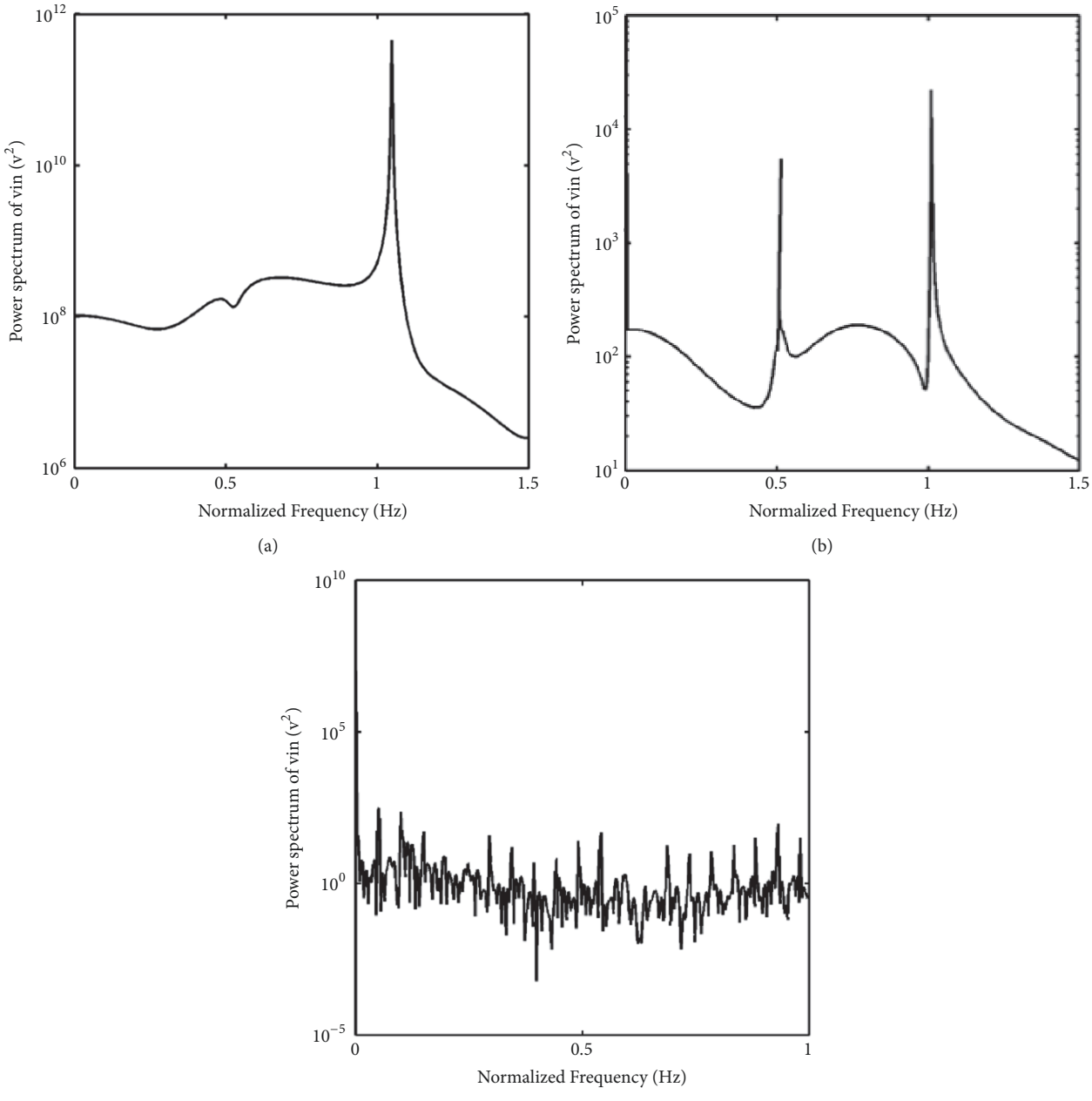

Figure 9: Power spectrum diagram of buck converter: (a) Phase 1; (b) Phase 2; (c) irregular phase.

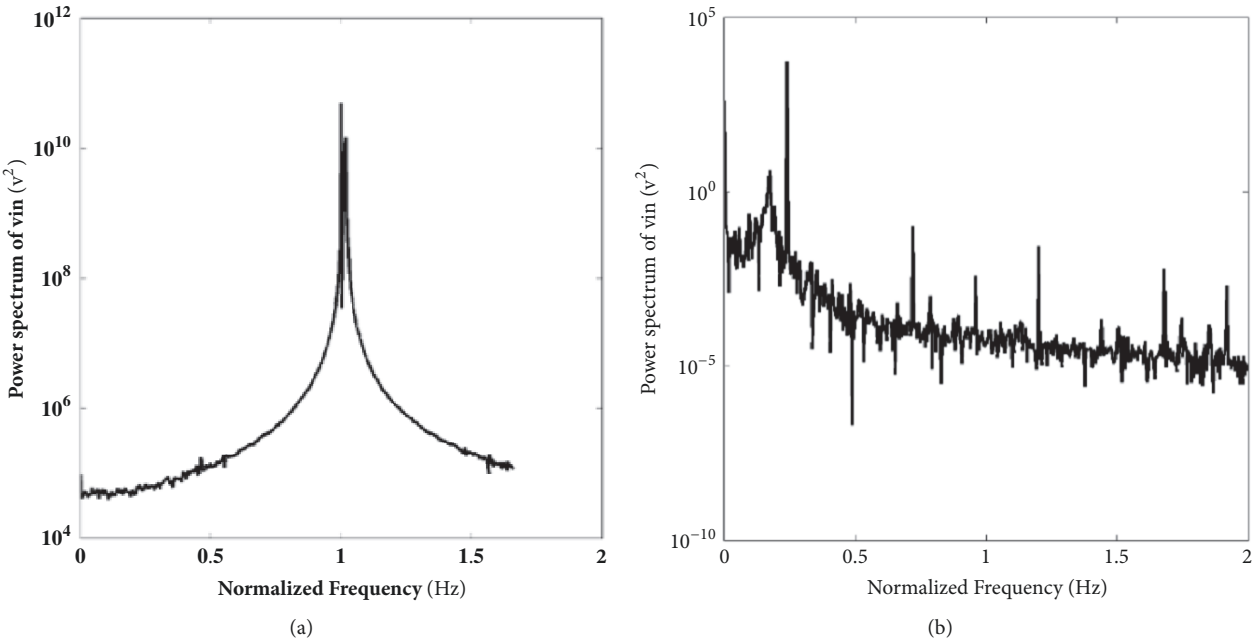

Figure 10: Power spectrum diagrams of buck converter: (a) Phase 1; (b) irregular phase.

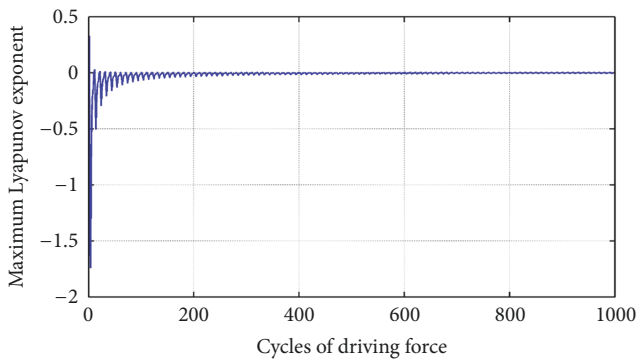

Figure 11: Diagram of Phase 1 Lyapunov exponent.

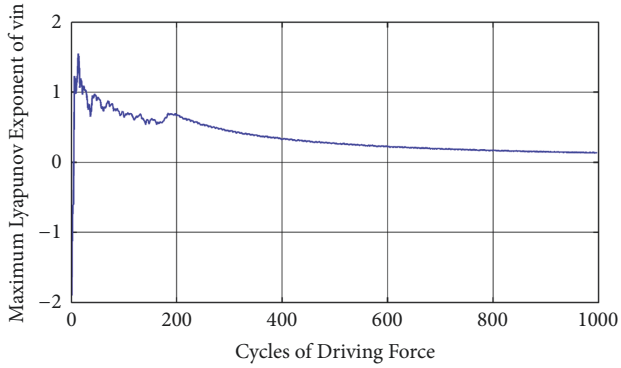

Figure 12: Diagram of the chaotic phase Lyapunov exponent.

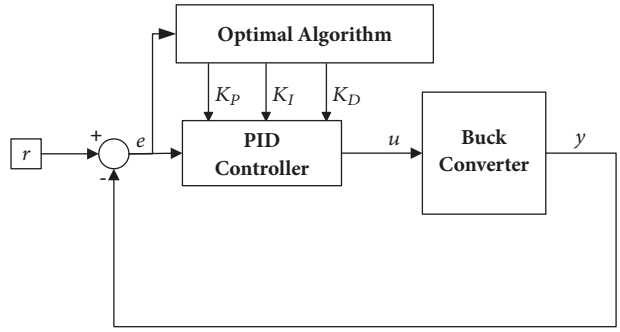

Figure 13: Block diagram of buck converter circuitry.

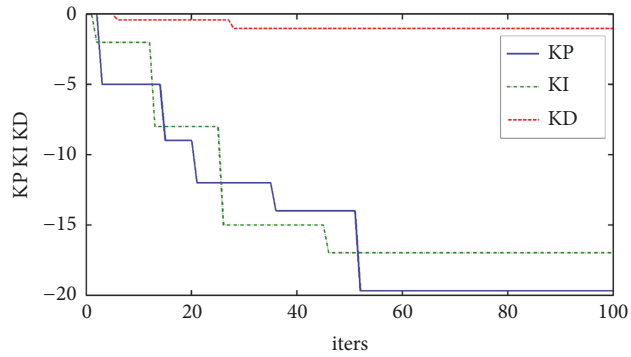

Figure 14: The genetic algorithm convergence curve of K_P, K_I, and K_D.

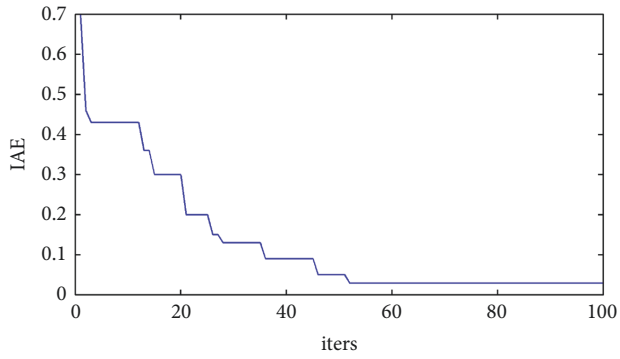

Figure 15: The genetic algorithm IAE curve.

chaotic state (40V). From Figure 11 it can be seen that after stabilization the curve is close to 0 and shows stability.

Figure 12 shows a Lyapunov diagram of the chaotic phase with the curve lying above zero after stabilization indicating the system is chaotic.

4. Optimized Control

In this study, Integral Absolute Error (IAE) was used as the adaption coefficient, as shown in Equation (5). The genetic algorithm was introduced to identify the parameters of the PID controller, K_P, K_I, and K_D. Figure 19 is a diagram of conditions after the establishment of PID control. The PID control parameters were acquired using the genetic algorithm: K_P= -19.67, K_I= -16.98, and K_D= -1.02. The genetic algorithm convergence curve in Figure 20 identifies K_P, K_I, and K_D after several iterations. Figure 21 shows and equivalent IAE curve of K_P, K_I, and K_D.

$$IAE = \int_0^\infty |e(t)|\, dt \tag{5}$$

Figure 13 is control block diagram of the system where u is input control source of the system, e is the system error, u is system control option, and y is system output.

The genetic algorithm [17, 18] finds the optimized parameter values after several iterations and then converges (see Figure 14). Figure 15 shows the IAE convergence curve.

The particle swarm optimization algorithm [19, 20] finds the optimized parameter values after several iterations: K_P= -20.6112, K_I= -25.3143, and K_D= -0.514; see Figure 16.

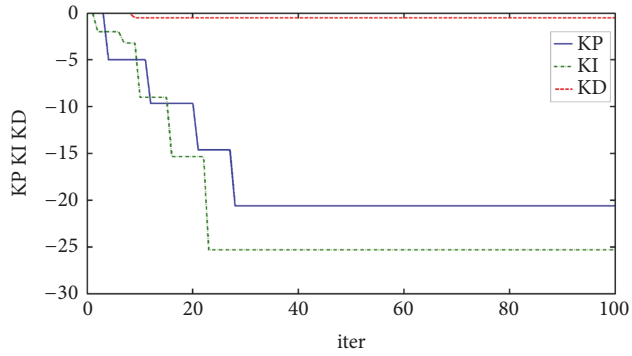

Figure 16: The particle swarm optimization algorithm convergence curve of K_P, K_I, and K_D.

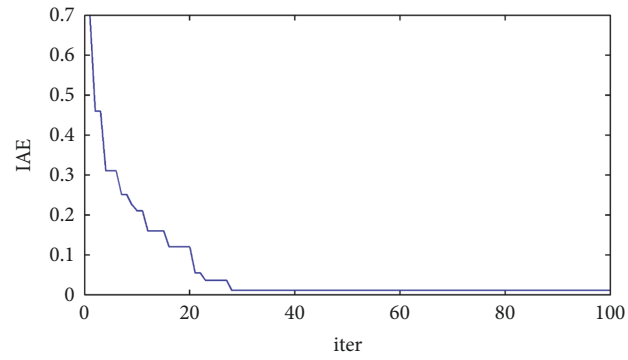

Figure 17: The particle swarm optimization algorithm IAE curve.

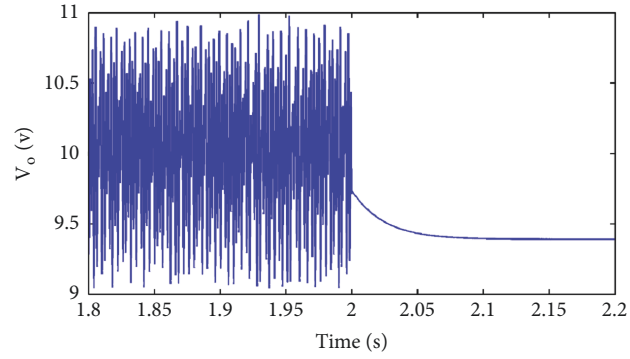

Figure 18: V_o after adding PID control.

Figures 15 and 17 show that the particle swarm optimization algorithm works better than the gene algorithm, and the PID parameter values identified by PSO are closer to optimal.

Figure 18 is the voltage wave diagram acquired after introducing and acquired from the PID controller optimization algorithm, where PID control starts after 2 seconds. It is clear from the diagram that the voltage becomes stable soon after the addition of control. Figure 19 shows the phase plane diagram after the start of control and the red line shows the curve after control had been established.

An optimization algorithm was used to identify the best parameters for PID and fussy control. Figure 20(a) shows a block diagram after fuzzy control had been applied and Figure 20(b) shows the membership functions screen of the fuzzy controller [21–23].

Figure 21 shows the output voltage curve 2 seconds after fuzzy control had been added. It is clear from the diagram that the voltage becomes stable soon after the addition of control. Figure 22 is the phase plane diagram after the start of control, and the red line shows the curve after control had been added.

Figure 23(a) shows a trace of the circuit output voltage at 40V, and the situation is clearly chaotic. Figure 23(b) shows the voltage trace after the addition of PID control, and a comparison with Figure 24 shows that fuzzy control is more effective than traditional PID control.

5. Conclusion

In this study, phase plane diagrams were used to verify the system status cycle and chaos phenomena. At the same time,

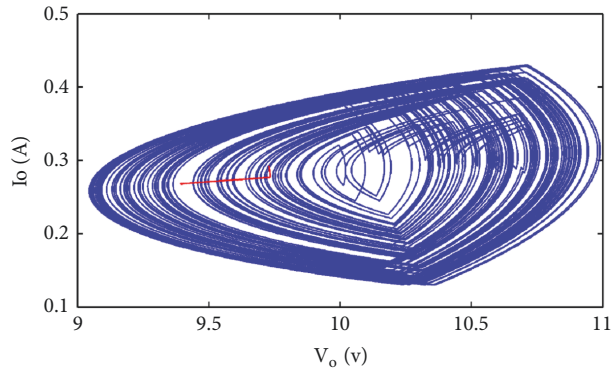

Figure 19: The phase plane diagram after adding PID control.

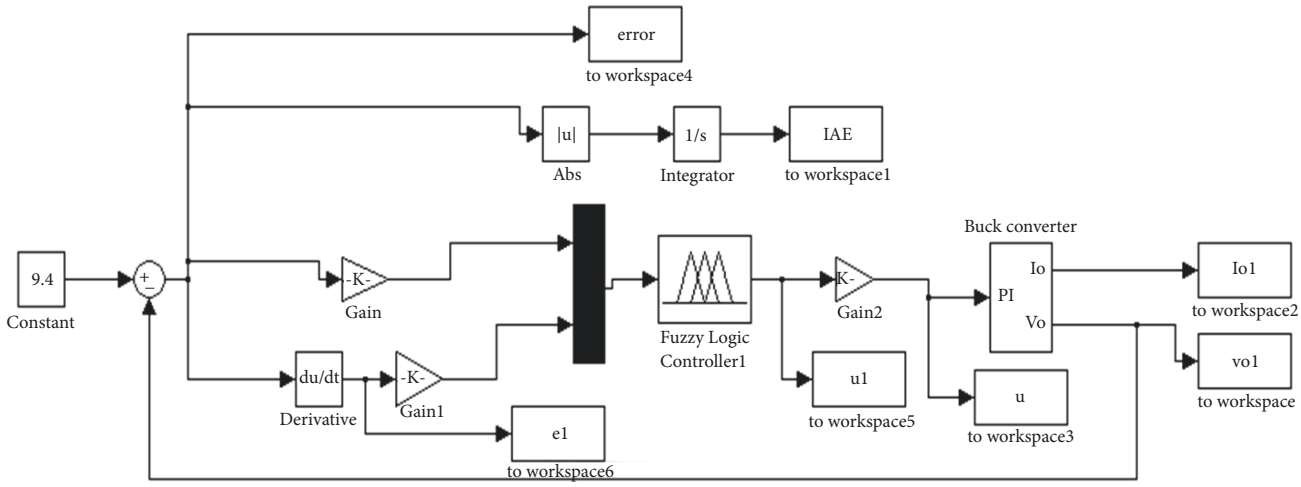

(a)

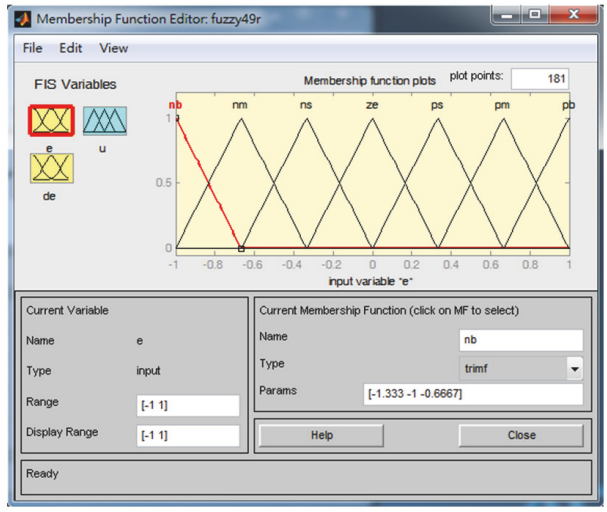

(b)

Figure 20: Block diagram after the addition of fuzzy control. (b). Membership functions screen.

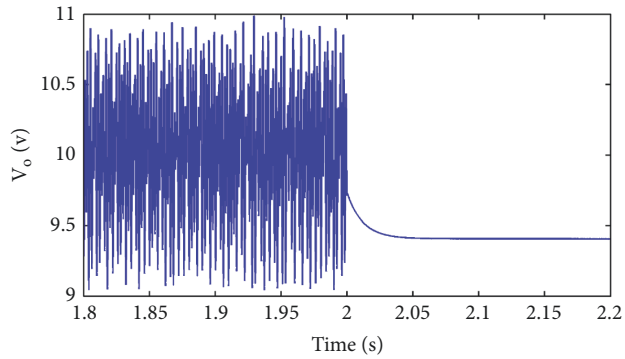

FIGURE 21: Voltage wave diagram after fuzzy control had been added.

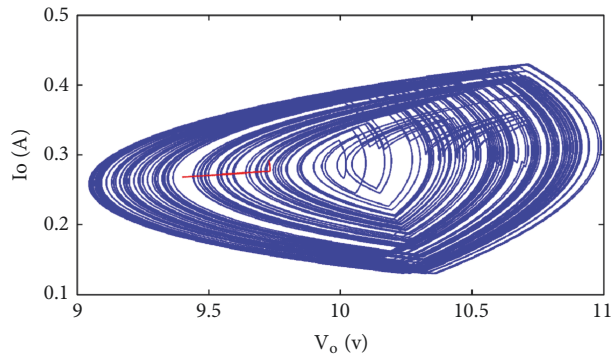

FIGURE 22: Phase plane diagram after fuzzy control had been added.

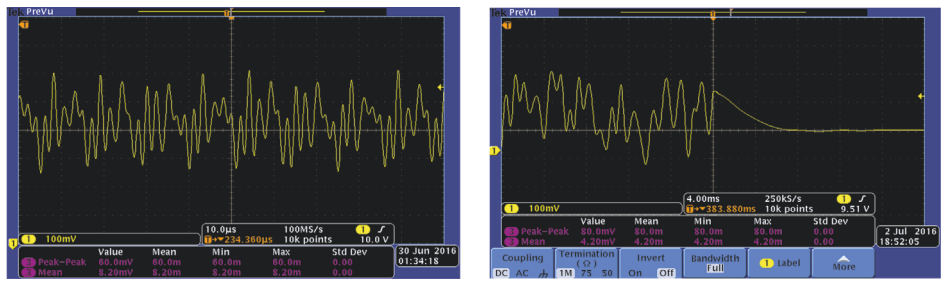

(a) (b)

FIGURE 23: (a) The chaotic output voltage of the circuit. (b). Output voltage after control has been added.

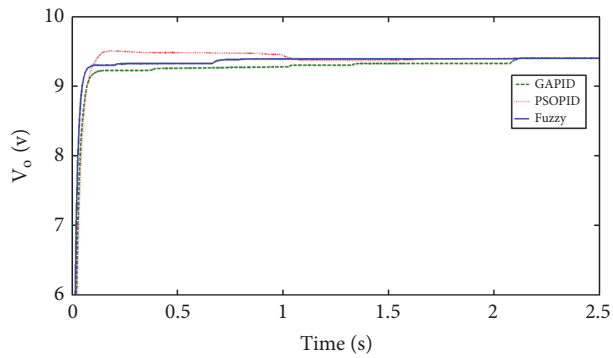

FIGURE 24: Comparison of GA, PSO, and fuzzy control.

stricter mathematical definitions and the largest Lyapunov exponent were used for system verification. This proved that, under special conditions, a DC-DC converter and the system will exhibit chaotic phenomena. Although the dynamic status falls within the stable strange attractor status, this is not desirable behavior for such a physical system. Logistic mapping was used to improve PSO, inhibit chaos, and control PID parameters. The experimental results showed that the method used here is very effective and can achieve faster convergence than other methods. In this study, optimization algorithms were used to identify gain values of PID controller parameters and PSO and GA were included. IAE was used as an adaption coefficient. A comparison of two algorithm methods showed that PSO works more effectively than GA. After fuzzy control was added the buck converter simulations showed that all three methods would allow the buck converter to reach stability. However, DSpace experiments with PID and fussy control showed fuzzy control to be better than PID.

Data Availability

The data used to support the findings of this study are available from the corresponding author upon request.

Conflicts of Interest

The authors declare no conflicts of interest.

Acknowledgments

Financial support of this research from the Ministry of Science and Technology, Taiwan, under Projects nos. 106-2218-E-167-001 and 106-2622-E-167-020-CC3 is gratefully acknowledged. The authors also would like to acknowledge, with thanks, comments from ICCPE&ICI for All MNHTE Workshop SPINTECH. This study has also gained from comments made at the poster workshop. This research project also received financial support from the Yunnan Province Science and Technology Department and Education Department Project of China (2017FH001-067, 2017FH001-117, and 2016ZDX127)

References

[1] E. Fossas, "Study of chaos in the buck converter," *IEEE Transactions on Circuits and Systems I: Fundamental Theory and Applications*, vol. 43, no. 1, pp. 13–25, 1996.

[2] C. K. Tse, Y. M. Lai, and H. H. C. Lu, "Hopf bifurcation and chaos in a free-running current-controlled Cuk switching regulator," *IEEE Transactions on Circuits and Systems I: Fundamental Theory and Applications*, vol. 47, no. 4, pp. 448–457, 2000.

[3] S. Parui and S. Banerjee, "Bifurcations due to transition from continuous conduction mode to discontinous conduction mode in the boost converter," *IEEE Transactions on Circuits and Systems I: Fundamental Theory and Applications*, vol. 50, no. 11, pp. 1464–1469, 2003.

[4] K. Chakrabarty, G. Poddar, and S. Banerjee, "Bifurcation behavior of the buck converter," *IEEE Transactions on Power Electronics*, vol. 11, no. 3, pp. 439–447, 1996.

[5] B. Allaoua and A. Laoufi, "Application of a robust fuzzy sliding mode controller synthesis on a buck-boost DC-DC converter power supply for an electric vehicle propulsion system," *Journal of Electrical Engineering & Technology*, vol. 6, no. 1, pp. 67–75, 2011.

[6] W. C. Chan and C. K. Tse, "Study of bifurcations in current-programmed dc/dc boost converters: from quasi-periodicity to period-doubling," *IEEE Transactions on Circuits and Systems I: Fundamental Theory and Applications*, vol. 44, no. 12, pp. 1129–1142, 1997.

[7] A. S. Oshaba, E. S. Ali, and S. M. Abd Elazim, "ACO based speed control of SRM fed by photovoltaic system," *International Journal of Electrical Power & Energy Systems*, vol. 67, pp. 529–536, 2015.

[8] A. S. Oshaba, E. S. Ali, and S. M. Abd Elazim, "MPPT control design of PV system supplied SRM using BAT search algorithm," *Sustainable Energy, Grids and Networks*, vol. 2, pp. 51–60, 2015.

[9] J. Chen, H. Yau, and J. Lu, "Implementation of FPGA-Based Charge Control for a Self-Sufficient Solar Tracking Power Supply System," *Applied Sciences*, vol. 6, no. 2, p. 41, 2016.

[10] C. Hsieh, H. Yau, C. Wang, and Y. Hsieh, "Particle swarm optimization used with proportional–derivative control to analyze nonlinear behavior in the atomic force microscope," *Advances in Mechanical Engineering*, vol. 8, no. 9, p. 168781401666727, 2016.

[11] J. Kennedy and R. Eberhart, "Particle swarm optimization," in *Proceedings of the IEEE International Conference on Neural Networks (ICNN '95)*, vol. 4, pp. 1942–1948, Perth, Western Australia, November-December 1995.

[12] J. H. Holland, *Adaptation in Natural and Artificial Systems: An Introductory Analysis with Applications to Biology, Control and Artificial Intelligence*, MIT Press, 1992.

[13] L. A. Zadeh, "Outline of new approach to the analysis of complex systems and decision processes," *IEEE Transactions on Systems, Man, and Cybernetics*, vol. 3, pp. 28–44, 1973.

[14] Y. Zhou, C. K. Tse, S.-S. Qiu, and F. C. M. Lau, "Applying resonant parametric perturbation to control chaos in the buck dc/dc converter with phase shift and frequency mismatch considerations," *International Journal of Bifurcation and Chaos*, vol. 13, no. 11, pp. 3459–3471, 2003.

[15] Y.-L. Zou, X.-S. Luo, and G.-R. Chen, "Pole placement method of controlling chaos in DC-DC buck converters," *Chinese Physics*, vol. 15, no. 8, pp. 1719–1724, 2006.

[16] F. Angulo, J. E. Burgos, and G. Olivar, "Chaos stabilization with TDAS and FPIC in a buck converter controlled by lateral PWM and ZAD," in *Proceedings of the 2007 Mediterranean Conference on Control and Automation, MED*, Greece, July 2007.

[17] N. Hussain, J. V, and M. Abraham, "Improving the Performance of Buck Converter PID Controller using Genetic Algorithm," in *Proceedings of the 8th SAEINDIA International Mobility Conference & Exposition and Commercial Vehicle Engineering Congress 2013 (SIMCOMVEC)*, 2013.

[18] X. Wang, M. Wu, L. Ouyang, and Q. Tang, "The application of GA-PID control algorithm to DC-DC converter," in *Proceedings of the 29th Chinese Control Conference, CCC'10*, pp. 3492–3496, China, July 2010.

[19] X. Li, M. Chen, and Y. Tsutomu, "A method of searching PID controller's optimized coefficients for Buck converter using particle swarm optimization," in *Proceedings of the 2013 IEEE 10th International Conference on Power Electronics and Drive Systems, PEDS 2013*, pp. 238–243, Japan, April 2013.

[20] S. A. Emami, M. B. Poudeh, and S. Eshtehardiha, "Particle swarm optimization for improved performance of PID controller on buck converter," in *Proceedings of the 2008 IEEE International Conference on Mechatronics and Automation, ICMA 2008*, pp. 520–524, Japan, August 2008.

[21] M. Ayati and Z. Sharifi, "Analysis and fuzzy control of chaotic behaviors in buck converter," in *Proceedings of the 4th International Conference on Control, Instrumentation, and Automation, ICCIA 2016*, pp. 319–323, Iran, January 2016.

[22] A. Abbasi, M. Rostami, J. Abdollahi, and H. R. Abbasi, "An analytical discrete model for evaluation the chaotic behavior of buck converter under current control mode," in *Proceedings of the 2009 IEEE Symposium on Industrial Electronics and Applications, ISIEA 2009*, pp. 112–116, Malaysia, October 2009.

[23] A. Perry, G. Feng, Y. Liu, and P. Sen, "A new design method for PI-like fuzzy logic controllers for DC-to-DC converters," in *Proceedings of the 2004 IEEE 35th Annual Power Electronics Specialists Conference*, pp. 3751–3757, Aachen, Germany, 2004.